NRC Research Press

ARTICLE

Adjacent functional group effects on the assembly of columnar liquid crystals

Carson O. Zellman, Danielle Vu, and Vance E. Williams

Abstract: Although the impact of individual functional groups on the self-assembly of columnar liquid crystal phases has been widely studied, the effect of varying multiple substituents has received much less attention. Herein, we report a series of dibenzo[*a*,*c*]phenazines containing an alcohol or ether adjacent to an electron-withdrawing ester or acid. With one exception, these difunctional mesogens form columnar phases. The phase behavior appeared to be dominated by the electron-withdrawing substituent; transition temperatures were similar to derivatives with these groups in isolation. In most instances, the addition of an electron-donating group *ortho* to an ester or acid suppressed the melting temperature and elevated the clearing temperature, leading to broader liquid crystal thermal ranges. This effect was more pronounced for derivatives functionalized with longer chain hexyloxy groups. These results suggest a potential strategy for controlling the phase ranges of columnar liquid crystals and achieving room temperature mesophases.

Key words: supramolecular chemistry, liquid crystal, physical organic chemistry, self-assembly.

Résumé : Bien que l'effet des groupes fonctionnels, pris individuellement, sur l'autoassemblage des phases colonnaires de cristaux liquides ait été largement étudié, l'effet d'une variation de plusieurs substituants à la fois a beaucoup moins retenu l'attention. Dans le présent article, nous présentons une série de dibenzo[*a*,*c*]phénazines comportant un substituant alcool ou éther adjacent à un groupe électroattracteur ester ou acide carboxylique. Tous ces mésogènes bifonctionnalisés, sauf un, forment des phases colonnaires. Le comportement des phases semble être dominé par le substituant électrodonneur; les températures de transition étant comparables à celles de dérivés dans lesquels ces groupes sont isolés. Dans la plupart des cas, l'ajout d'un substituant électrodonneur en position *ortho* par rapport à un groupe ester ou acide a éliminé la température de fusion et a élevé la température de clarification, ce qui a donné lieu à des plages de températures élargies de l'état cristal liquide. Cet effet était plus marqué pour les dérivés portant des groupes hexylhydroxy, dont la chaîne est plus longue. Ces résultats laissent entrevoir une stratégie pour moduler les plages thermiques des phases colonnaires des cristaux liquides et accéder à des mésophases à température ambiante. [Traduit par la Rédaction]

Mots-clés : chimie supramoléculaire, cristal liquide, chimie organique physique, autoassemblage.

Introduction

James Wuest has asserted that understanding molecular crystallization is one of the "great unmet challenges of contemporary science."[1] Although posed in the context of solids, this statement applies equally well to liquid crystals, which are exquisitely sensitive to variations at the molecular level.[2–5] As such, the introduction of structural changes to satisfy application-specific properties can have unpredictable and undesirable effects on the self-assembly process.[6–9] Delineating the rules that govern molecular organization is therefore critical for the design of new liquid crystal (LC) materials.

It is in this context that we have been examining the structure–property relations of columnar liquid crystals formed from disc-shaped molecules ("discotic mesogens"). These phases have been targeted for applications such as solar cells,[10–15] ferroelectrics,[16–18] and ionic conductive materials.[19–21] Our primary targets are dibenzophenazines, **D**(**X**,**Y**), which constitute a versatile family of discotic mesogens that tend to form columnar phases with wide temperature ranges.[22–26] Functional groups dramatically influence the self-assembly of these systems.[27–30] For instance, the methyl ester **D**(**MeE**,**H**) forms a broad columnar hexagonal (Col_h) phase,[31] whereas **D**(**H**,**OMe**) is not liquid crystalline.[32] These differences were ascribed to the stabilization of the columnar phase via π-stacking and dipole–dipole interactions, both of which are favored by electron-withdrawing groups such as esters.[33,34] Functional groups that engage in specific interactions such as hydrogen bonding further alter the stability of the LC phase; the clearing point of the carboxylic acid **D**(**CA**,**H**) is 60 °C higher than that of the corresponding methyl ester **D**(**MeE**,**H**).[31]

In the above examples, the functional groups being varied are relatively isolated; they lack adjacent substituents. Although we anticipate neighbouring groups would perturb the liquid crystal properties, it is difficult to predict the nature or magnitude of these changes. We have therefore undertaken the synthesis of a series of dibenzophenazine esters, **D**(**MeE**,**Y**), and carboxylic acids, **D**(**CA**,**Y**), bearing ortho-hydroxy, methoxy, or *n*-hexyloxy groups (Y = OH, OCH_3, OC_6H_{13}) (Fig. 1). These substituents were chosen both for their synthetic accessibility and to allow us to probe the effects of sterics and hydrogen bonding on the phase behavior. To better understand the role of hydroxy and hexyloxy groups independent of their impact on neighbour substituents, we also prepared the **D**(**H**,**OH**) and **D**(**H**,**OHx**) derivatives.

Received 6 February 2020. Accepted 17 April 2020.

C.O. Zellman, D. Vu, and V.E. Williams. Department of Chemistry, Simon Fraser University, Burnaby, BC V5A 1S6, Canada.
Corresponding author: Vance E. Williams (email: vancew@sfu.ca).

This paper is part of a special issue to honour Professor Jim Wuest.

Fig. 1. Dibenzophenazine derivatives studied in this paper. An asterisk indicates compounds that were reported elsewhere.[31,32,33]

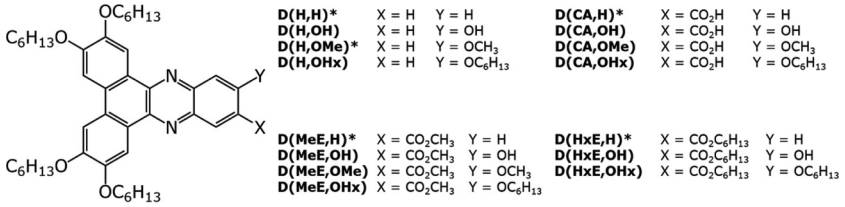

Scheme 1. Reagents and conditions: step a, palladium on carbon (Pd/C), hydrazine hydrate, ethanol, reflux, 3 h, >90%; step b, glacial acetic acid (cat.), ethanol, reflux, 12 h, 79%; step c, 1-bromohexane, Bu_4NBr (cat.), $CsCO_3$, butanone, reflux, 12 h, 75%.

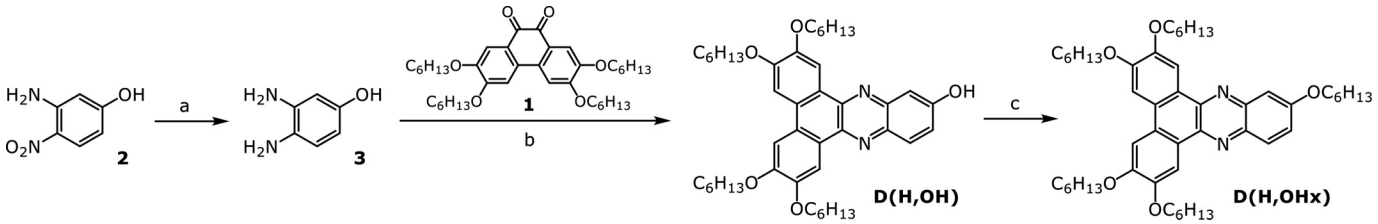

Scheme 2. Reagents and conditions: step a, concentrated sulfuric acid, methanol, 0 °C – reflux, 16 h, 88%; step b, bismuth(III)nitrate pentahydrate ($Bi(NO_3)_3{\cdot}5H_2O$), acetic anhydride, dry dichloromethane, room temperature, 3 h, 38%; step c, concentrated sulfuric acid, methanol, reflux, 16 h, 96%; step d, iron powder, concentrated hydrochloric acid, methanol, reflux, 1 h, 95%; step e, glacial acetic acid (cat.), ethanol, reflux, 16 h, 96%.

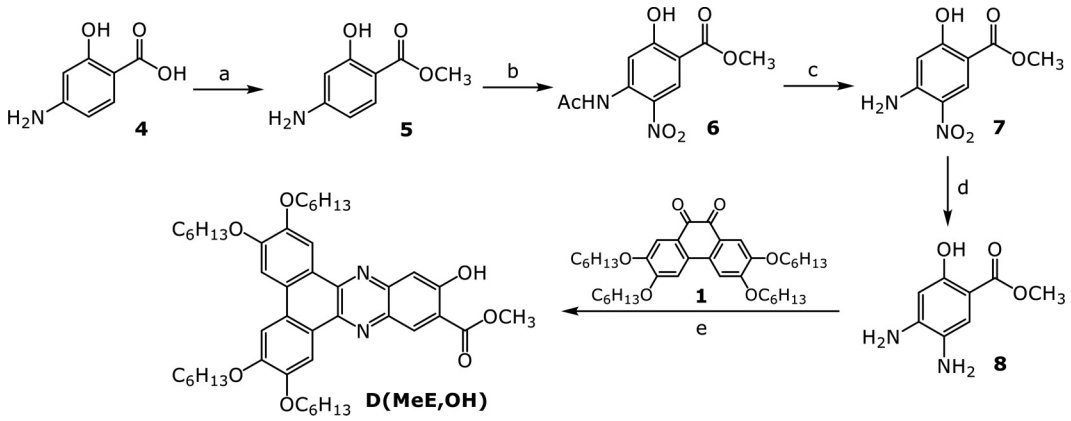

Results and discussion

Dibenzophenazines **D**(**X**,**Y**) are readily accessed through the condensation of appropriate 1,2-phenylenediamine with the phenanthrene quinone **1**; the synthesis of this quinone has been reported elsewhere.[23,26,35] The mono-functionalized **D**(**H**,**OH**) and **D**(**H**,**OHx**) derivatives were synthesized according to Scheme 1. Commercially available 4-amino-3-nitrophenol (**2**) was reduced to 3,4-diaminophenol (**3**) by hydrazine hydrate in the presence of catalytic palladium. This electron-rich diamine showed noticeable degradation on prolonged exposure to oxygen and was therefore prepared as needed and used without further purification. Following a previously reported condensation method,[31] reaction of this compound with **1** in ethanol and catalytic glacial acetic acid afforded the alcohol **D**(**H**,**OH**). Reaction of **D**(**H**,**OH**) with 1-bromohexane in the presence of catalytic tetrabutylammonium bromide (Bu_4NBr) and cesium carbonate (Cs_2CO_3) in butanone afforded **D**(**H**,**OHx**) in good yield (75%).

The synthesis of the remaining dibenzophenazines proceeded via the *ortho*-hydroxy methyl ester **D**(**MeE**,**OH**) (Schemes 2 and 3), which was obtained from condensation of **1** and the diaminosalicylate **8**; the latter was prepared using an approach adapted from He and coworkers (Scheme 1).[36] 4-Aminosalicylic acid (**4**) was converted in 88% yield to its methyl ester (**5**) via Fischer–Speier esterification. Using the one-pot procedure of Lu et al.,[37] this intermediate was N-acetylated and nitrated with a mixture of acetic anhydride and bismuth(III)nitrate pentahydrate ($Bi(NO_3)_3{\cdot}5H_2O$) to afford **6** in 38% yield. He and coworkers reported nitration of the acetanilide using a mixture of nitric and acetic acid;[36] however, in our hands, this nitration method gave inconsistent results, leading us to adopt the bismuth nitrate synthesis. The amide **6** was deacetylated with concentrated sulfuric acid in methanol to give **7**, which was then reduced using iron powder and concentrated hydrochloric acid to afford methyl 4,5-diamino-2-hydroxybenzoate (**8**) in excellent yield (95%). Reaction of **1** and **8** under the conditions described above give **D**(**MeE**,**OH**) in 96% yield.

The syntheses of the remaining dibenzophenazine esters and acids are shown in Scheme 3. The *ortho*-hydroxy acid, **D**(**CA**,**OH**), was prepared by hydrolysis of the parent ester **D**(**MeE**,**OH**) in a concentrated solution of sodium hydroxide in 1,4-dioxane. The *ortho*-alkoxy methyl ester derivatives, **D**(**MeE**,**OMe**) and **D**(**MeE**,**OHx**), were synthesized by base-catalyzed alkylation of **D**(**MeE**,**OH**) with the appropriate alkyl halide. Synthesis of the hexyloxy analogue **D**(**MeE**,**OHx**) was accompanied by the formation of 5%–10% of the *trans*-esterification side products **D**(**HxE**,**OH**) or **D**(**HxE**,**OHx**), likely due to residual water in the reaction solvent. The side-product **D**(**HxE**,**OH**) was only observed in reactions using potassium carbonate (K_2CO_3) in acetone; reactions with cesium carbonate (Cs_2CO_3) in butanone afforded **D**(**MeE**,**OHx**) and **D**(**HxE**,**OHx**) only, thus suggesting these

Scheme 3. Reagents and conditions: step a, $NaOH_{(aq)}$, 1,4-dioxane, reflux, 16 h, 64%; step b, methyl iodide, K_2CO_3, dimethylformamide, reflux, 16 h, 79%; step c, 1-bromohexane, Cs_2CO_3, Bu_4NBr, butanone, reflux, 16 h, 42%; step d, 1-bromohexane, K_2CO_3, Bu_4NBr (cat.), acetone, reflux, 16 h, 1%–2%; step e, $NaOH_{(aq)}$, EtOH, reflux, 16 h, 90%–99%.

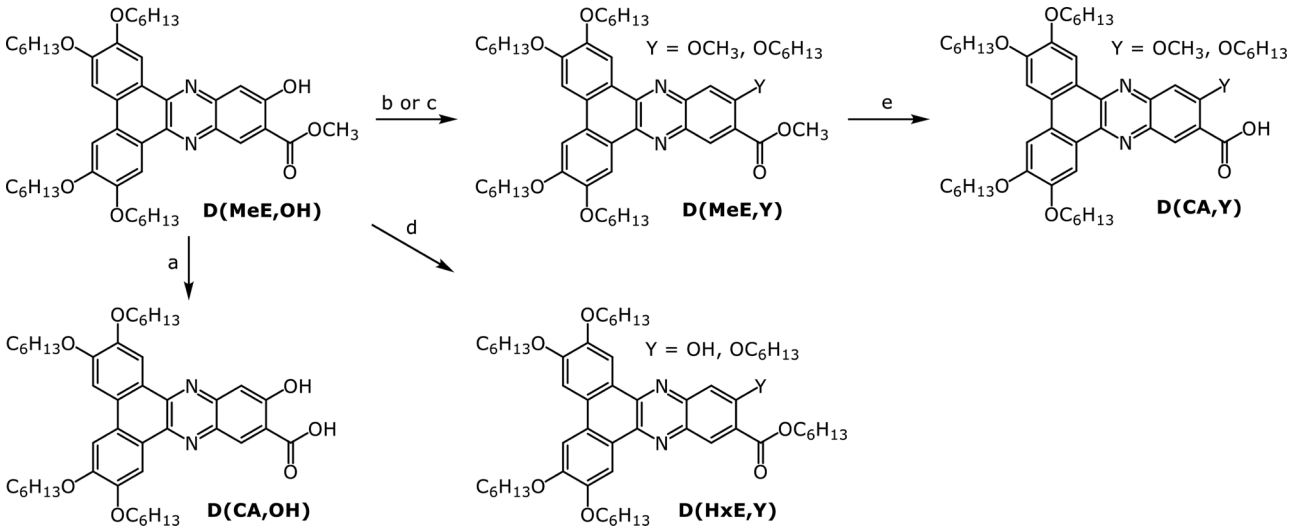

Table 1. Phase behaviour of compounds studied.

Compound	Phase	*T*, °C (Δ*H*/kJ mol⁻¹)	Phase	*T*, °C (Δ*H*/kJ mol⁻¹)	Phase	*T*, °C (Δ*H*/kJ mol⁻¹)	Phase
D(H,OH)	Cr	247.1 (50.3) 217.5 (-32.9)	Iso				
D(H,OHx)	Cr	96.9 (38.0) 42.0 (-31.6)	Col_h	110.4 (0.9) 103.7 (-1.6)	Iso		
D(CA,OH)	Cr	242.8 (27.5) 222.9 (-32.6)	Iso				
D(CA,OMe)	Cr	142.0 (17.5)	Col_h	203.4 (4.4) 200.6 (-4.6)	Iso		
D(CA,OHx)	Cr	74.3 (11.4)	Col_r	129.5 (12.3) 105.2 (-9.7)	Col_h	222.4 (4.6) 220.5 (-4.7)	Iso
D(MeE,OH)	Cr	125.3 (34.0) 90.9 (-34.1)	Col_h	193.1 (3.9) 191.5 (-3.6)	Iso		
D(MeE,OMe)	Cr	108.6 (27.3)	Col_h	210.6 (2.8) 206.7 (-4.3)	Iso		
D(MeE,OHx)	Cr	85.5 (26.8)	Col_h	221.3 (6.5) 219.9 (-6.6)	Iso		
D(HxE,OH)	Cr	74.5 (23.6) 3.9 (-8.2)	Col_h	190.0 (3.3) 187.1 (-4.3)	Iso		
D(HxE,OHx)	Cr	44.2 (25.6) -11.3 (-11.0)	Col_h	206.5 (6.8) 205.3 (-6.9)	Iso		

Note: Phase: Cr, crystalline; Col_h, columnar hexagonal; Iso, isotropic. Transition temperatures and enthalpies were determined by differential scanning calorimetry (DSC) (scan rate = 10 °C/min) on second heating run, except for **D(CA,OHx),** which was taken from its first heating run.

conditions provided more efficient alkylation. The *trans*-esterification impurities, **D(HxE,OH)** and **D(HxE,OHx)**, were isolated and their LC properties also investigated, as discussed below.

The esters **D(MeE,OMe)** and **D(MeE,OHx)** were hydrolyzed under basic conditions to the corresponding acids **D(CA,OMe)** and **D(CA,OHx)**, respectively, in excellent yields. In the latter case, it was not necessary to remove the hexyl ester impurity **D(HeE,OHx)** from **D(MeE,OHx)**, as both hydrolyze to **D(CA,OHx)**.

The LC properties for the newly prepared compounds were characterized by differential scanning calorimetry (DSC), polarized optical microscopy (POM), and variable temperature powder X-ray diffraction (VT-pXRD) experiments. The results from these experiments are summarized in Tables 1 and 2. All compounds show reproducible phase transitions on consecutive heating–cooling cycles, with the exception of those that supercool from their LC phases (see below), which do not exhibit melting transitions on the second or subsequent heating scans. No signs of degradation up to 250 °C were observed.

With the exceptions of **D(H,OH)** and **D(CA,OH)**, which both melt directly from solids into isotropic liquids, the newly prepared compounds all possess enantiotropic LC phases (Table 1). DSC endotherms for these compounds exhibit a large enthalpy peak at low temperatures and a smaller peak at higher temperatures, which were ascribed to crystalline to LC (melting) and LC to

Table 2. X-ray diffraction data and lattice constants for **D**(**X**,**Y**) compounds.

	T (°C)	d-spacing (Å)	Miller index (hkl)	Phase (lattice constants)
D(H,OH)	25		Crystalline solid	
D(H,OHx)	66	18.0	(100)	Col_h (a = 20.8 Å)
		4.5	Alkyl halo	
		3.4	π–π stacking	
D(CA,OH)	25		Crystalline solid	
D(CA,OMe)	180	17.3	(100)	Col_h (a = 19.9 Å)
		3.5	π–π stacking	
D(CA,OHx)	189	18.5	(100)	Col_h (a = 21.4 Å)
		4.8	Alkyl halo	
		3.5	π–π stacking	
	25	19.9	(200)	Col_r (a = 39.7 Å) (b = 17.6 Å)
		16.1	(110)	
		10.9	(310)	
		8.8	(020)	
		8.0	(220)	
		4.2	Alkyl halo	
		3.4	π–π stacking	
D(MeE,OH)	175	17.4	(100)	Col_h (a = 20.1 Å)
		4.6	Alkyl halo	
		3.5	π–π stacking	
D(MeE,OMe)	131	17.5	(100)	Col_h (a = 20.2 Å)
		4.2	Alkyl halo	
		3.5	π–π stacking	
D(MeE,OHx)	199	18.9	(100)	Col_h (a = 21.8 Å)
		4.5	Alkyl halo	
		3.5	π–π stacking	
D(HxE,OH)	147	18.4	(100)	Col_h (a = 21.3 Å)
		4.6	Alkyl halo	
		3.5	π–π stacking	
D(HxE,OHx)	163	19.6	(100)	Col_h (a = 22.6 Å)
		4.6	Alkyl halo	
		3.5	π–π stacking	

isotropic liquid (clearing) transitions, respectively (Fig. 2*a*; Supplementary Figs. S1–S5). The higher temperature peaks show minimal hysteresis on cooling, consistent with LC–isotropic transitions. Slow cooling from the isotropic phase leads to the formation of dendritic textures with six-fold symmetry under polarized optical microscopy (Figs. 3*a*, 3*b*, 4*a*, and 4*b*; Supplementary Figs. S7 and S9–S14), characteristic of a columnar hexagonal (Col_h) liquid crystal. Mechanical shearing confirmed the fluidity of these samples. These samples have a strong tendency to homeotropically align in POM experiments, a common feature of dibenzophenazine mesogens.[26,33]

VT-pXRD studies are consistent with the assignment of Col_h phases (Table 2). Diffraction patterns show a single sharp intense peak at low angles, which is assigned to the (100) diffraction of a hexagonal lattice. In the higher angle region, two broad peaks appear at around 4.5 Å and 3.5 Å, assigned to the packing of the alkyl chains and between the aromatic cores, respectively (Fig. 2*b*; Supplementary Figs. S16 and S18–S23). Changes in the functional groups have a small impact on the intercolumnar distance, *a*, which suggests that all derivatives pack in a similar manner in the LC phase. It is probable that, like previously reported dibenzophenazines, these mesogens adopt an antiparallel arrangement within the columns.[28,32]

Although most compounds exhibited a single LC phase, **D**(**CA**,**OHx**) forms a second, low-temperature mesophase above the melting temperature. Under POM, a clear transition is observed upon cooling below 105 °C (Fig. 4*c*); the sample develops striations and then rapidly becomes uniformly birefringent. Tentative assignment of this phase as a columnar rectangular (Col_r) phase was confirmed by VT-pXRD. Above 105 °C, this compound shows a diffraction pattern consistent with a Col_h phase, as described above. Below this transition, the (100) splits into two intense diffractions that were assigned to the (200) and (110) peaks of a rectangular phase. Additional low intensity peaks also developed, which were indexed to (310), (020), and (220) of the two-dimensional rectangular lattice (Supplementary Fig. S19).

Most compounds exhibited a large depression of the LC–crystal transition with respect to the corresponding melting transitions observed on heating. In DSC experiments, this hysteresis was as large as 107 °C. For **D**(**MeE**,**OMe**), **D**(**MeE**,**OHx**), **D**(**CA**,**OMe**), and **D**(**CA**,**OHx**), no freezing transition was observed down to –40 °C by DSC. **D**(**MeE**,**OHx**) undergoes a melting transition on subsequent heating cycles, indicating that crystallization takes place during the short intervals between DSC runs. In the cases of **D**(**MeE**,**OMe**) and **D**(**CA**,**OMe**), cold crystallization was observed on subsequent DSC runs prior to the crystalline to LC melting transition. **D**(**CA**,**OHx**) shows neither a melting transition nor a cold crystallization on subsequent heating cycles, indicating that crystallization does not occur on the timescale between DSC runs.

Most compounds were observed to crystallize on short timescales in POM experiments, forming highly birefringent grain-like or needle-like textures upon cooling. This was confirmed by room temperature XRD experiments, which showed numerous sharp peaks, indicative of crystalline solid phases. Crystallization of **D**(**MeE**,**OHx**) occurs within an hour, consistent with the DSC experiments described above. POM observations of **D**(**MeE**,**OMe**), which undergoes cold crystallization by DSC, indicate that this compound crystallizes at room temperature over the timescale of

Fig. 2. (*a*) DSC endotherm for the second heating and cooling cycle of **D**(**MeE**,**OH**) (heating/cooling rate = 10 °C/min). (*b*) X-ray diffractogram of **D**(**MeE**,**OH**) at 175 °C.

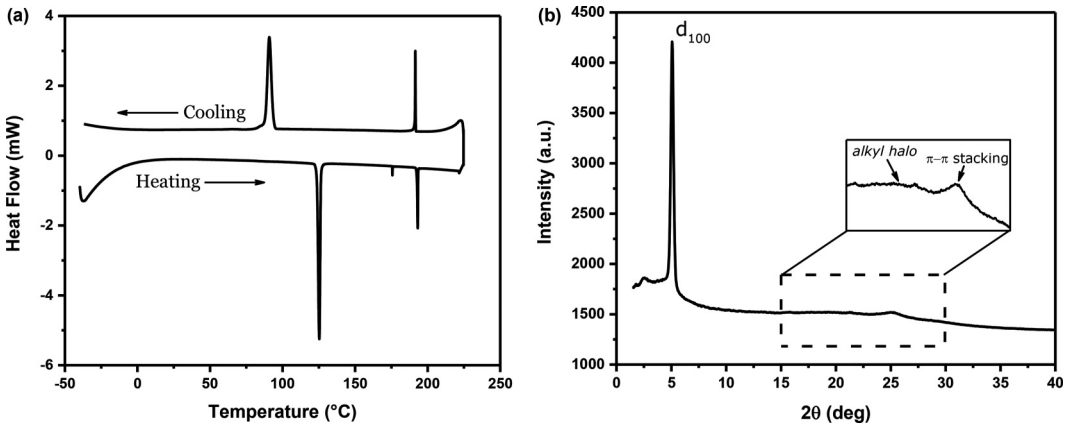

Fig. 3. Polarized optical micrographs of **D**(**MeE**,**OMe**) at 204 °C (*a*) with and (*b*) without a 530 nm quarter wave plate. Both images were taken in the same plane of view. [Colour online.]

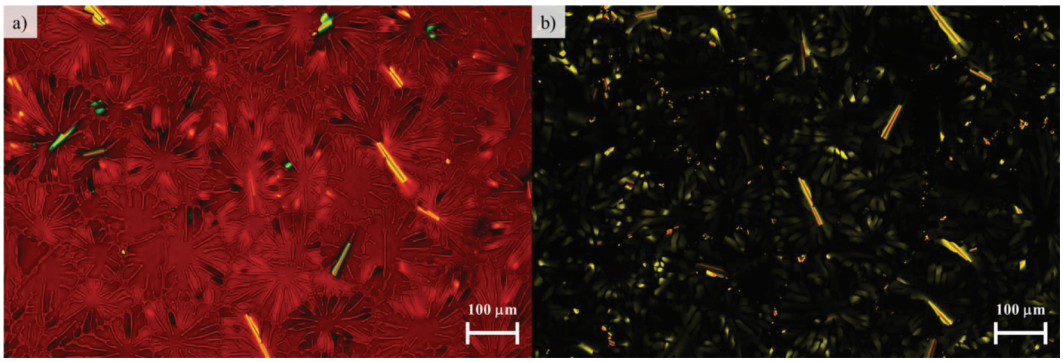

Fig. 4. Polarized optical micrographs of **D**(**CA**,**OHx**) at 206 °C (*a*) with and (*b*) without a 530 nm quarter wave plate, at (*c*) 100 °C and at (*d*) room temperature after 1 month. Images (*a*), (*b*), and (*c*) were taken in the same plane of view. [Colour online.]

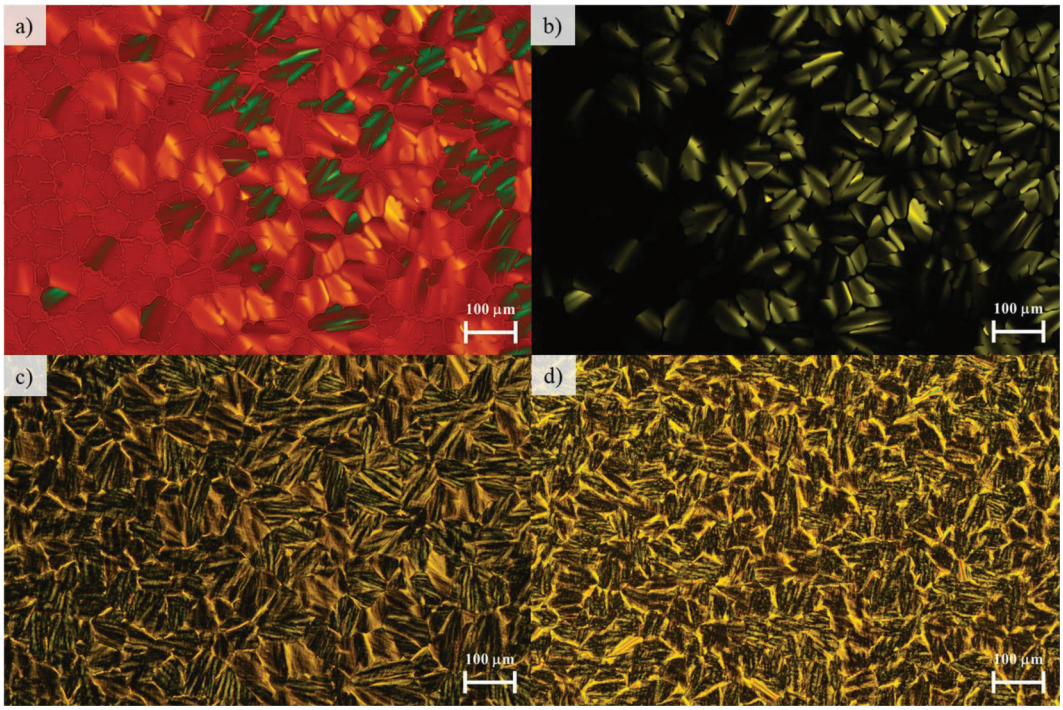

Fig. 5. Graphical representation of the phase ranges of **D(X,H)** and **D(H,Y)** series: Cr (gray), Col_h (blue), and Iso (white). [Colour online.]

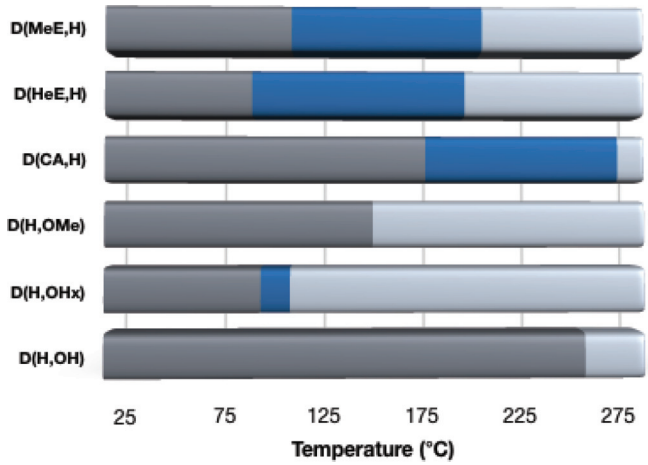

Fig. 6. Graphical representation of the phase ranges of **D(MeE,Y)** series: Cr (gray), Col_h (blue), and Iso (white). [Colour online.]

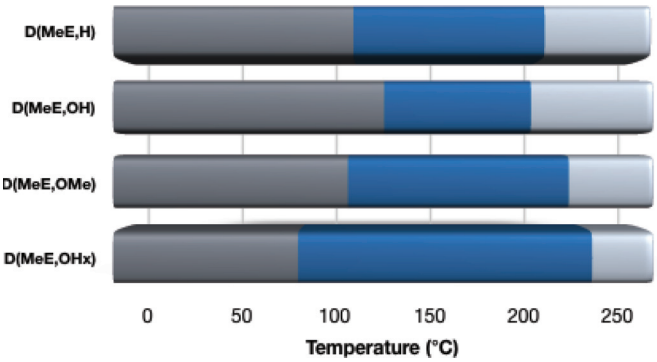

a few months. No crystallization was observed for **D(CA,OMe)** and **D(CA,OHx)** even after almost a year at room temperature (Fig. 4*d*; Supplementary Fig. S9); instead, they retain LC domain ordering.

Before discussing the effects of adjacent functional groups, it is first worth examining the phase behaviour of the six derivatives, **D(CA,H)**, **D(MeE,H)**, **D(HxE,H)**, **D(H,OH)**, **D(H,OMe)**, and **D(H,OHx)**, that bear each of these functional groups in isolation. The phase sequences of these compounds are shown schematically in Fig. 5. The previously reported electron-deficient esters **D(MeE,H)**[31] and **D(HxE,H)**[33] have elevated clearing temperatures and broad columnar phases. The phase range of the electronically similar carboxylic acid, **D(CA,H)**, is shifted to higher temperatures, likely because of the ability of these groups to hydrogen bond.[31] In contrast, the electron-rich methyl ether **D(H,OMe)** is non-liquid crystalline. The newly prepared hexyloxy derivative **D(H,OHx)** exhibits a narrow Col_h phase, with a clearing temperature that is more than 80 °C lower than either of the esters, in keeping with previous observations that electron-withdrawing groups elevate this transition.[32] The observation of an LC phase for **D(H,OHx)**, but not for the electronically similar compound **D(H,OMe)**, can be attributed to the depression of the former's melting point. The hydroxy-substituted derivative **D(H,OH)** also fails to form a columnar LC phase, likely because its anomalously high melting point (247 °C) lies well above the clearing temperature expected for an electron-rich mesogen.

Because the parent ester and acid derivatives form broad liquid crystal phases, our initial analysis focuses on the perturbation of these phase ranges by adjacent groups. The phase sequences of the methyl esters are shown in Fig. 6. Surprisingly, although we

Fig. 7. Graphical representation of the phase ranges of **D(HxE,Y)** series: Cr (gray), Col_h (blue), and Iso (white). [Colour online.]

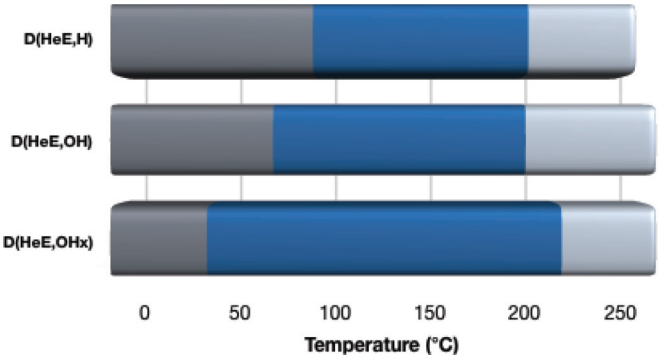

Fig. 8. Graphical representation of the phase ranges of **D(CA,Y)** series: Cr (gray), Col_h (blue), Col_r (red), and Iso (white). [Colour online.]

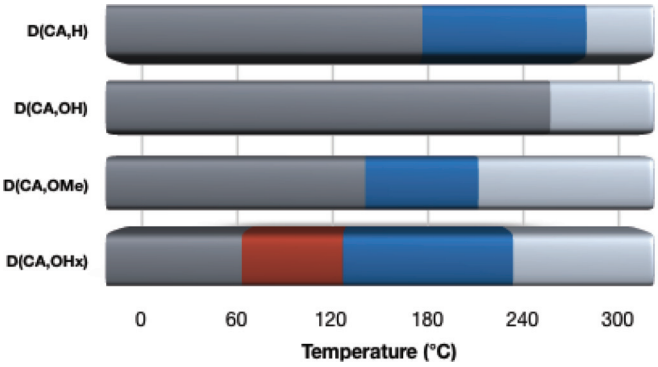

anticipated that the addition of an electron-donating ether would destabilize the phases, the opposite effect is observed, with both the methoxy, **D(MeE,OMe)**, and hexyloxy, **D(MeE,OHx)**, derivatives clearing at 10–20 °C higher than the parent compound **D(MeE,H)**. A similar effect is seen for the hexyl ester series (Fig. 7); the clearing temperature of **D(HxE,OHx)** is approximately 15 °C higher than that of its parent, **D(HxE,H)**. We speculate that this stabilization is due to the ability of the ether group to effectively fill space within the material.[38] At the same time, these bifunctional mesogens also melt at lower temperatures, resulting in liquid crystal phase ranges that are appreciably broadened. This effect is especially pronounced for **D(HxE,OHx)**, which exhibits a Col_h phase over a span of more than 160 °C, compared with **D(HxE,H)**, which has an approximately 100 °C phase range. Notably, the nearly 50 °C depression of the melting point of **D(HxE,OHx)** brings its liquid crystal phase close to room temperature, which is particular attractive for practical applications.

Although ether groups stabilize the mesophases of the esters, they have the opposite effect on the carboxylic acids (Fig. 8). The parent acid, **D(CA,H)**, has a clearing temperature of 262.5 °C; this value drops dramatically to 222 °C for the hexyl ether **D(CA,OHx)** and 203.5 °C for the methoxy derivative **D(CA,OMe)**. As already noted, the clearing temperature of the carboxylic acid **D(CA,H)** is much higher than that of the corresponding esters, **D(HxE,H)** and **D(MeE,H)**, likely due to the formation of hydrogen bonded dimers. The presence of groups ortho to the acid may prevent these intermolecular interactions, either through competing intramolecular hydrogen bonding or because of steric hindrance. Notably, the clearing temperatures of these acids, **D(CA,OMe)** and **D(CA,OHx)**, are very close to those of the corresponding methyl esters **D(MeE,OMe)** and **D(MeE,OHx)**, which we would expect if the acids' ability dimerize were impeded.

The impact of phenol groups varies considerably across the compounds studied. Their effects on the phase behavior of esters are comparatively modest: **D(MeE,OH)** possesses a slightly narrower mesophase than its parent ester, **D(MeE,H)**, with a lower clearing temperature and an elevated melting temperature. In contrast, **D(HxE,OH)** and **D(HxE,H)** clear at approximately the same temperature, but the former exhibits a slightly lower melting temperatures and a broader LC phase range. The melting points of **D(MeE,OH)** (125 °C) and **D(HxE,OH)** (75 °C) are in stark contrast to those of the monosubstituted phenol **D(H,OH)** and the carboxylic acid derivative **D(CA,OH)**, which melt directly into their isotropic state at 246 °C and 243 °C, respectively. We speculate that the high melting points of these last two compounds are due to hydrogen bonding between mesogens, which is inhibited by the presence of bulky ester groups in the cases of **D(MeE,OH)** and **D(HxE,OH)**.

Overall, our observations suggest that the clearing temperatures of these mixed-functional group systems tend to be governed by the more electron-withdrawing substituent; the clearing temperature is generally much closer to that of the parent acid or ester than its ether or alcohol parent. For example, **D(H,OHx)** has a clearing temperature of 110.4 °C, whereas the mesogenic ester and acid derivatives all clear in excess of 190 °C. Thus, these carbonyl groups seem to dominate mesophase stability. However, the perturbations induced by ether or alcohol groups can be substantial; the clearing temperature of **D(CA,OMe)** is almost 60 °C lower than its parent acid **D(CA,H)**, whereas **D(MeE,OHx)** clears more than 20 °C higher than **D(MeE,H)**. Melting points are likewise strikingly sensitive to the introduction of ether groups, which in most cases led to a lowering of this transition.

Conclusion

In the present work, we investigated the effects of adjacent functional groups on the phase behavior of discotic mesogens. We found that functional group effects are not strictly additive, namely the impact of a group depends on its neighbour. The effects are likely due to the interplay of electronic perturbations on the core, as well as the ability of groups to effectively fill space within the material. In the case of hydrogen-bonding groups such as hydroxyl and carboxylic acids, adjacent functional groups appear to destabilize the phases, presumably by inhibiting intermolecular H-bonds. The addition of ethers to ester derivatives has the opposite effect of raising the clearing point. At the same time, these compounds melt at lower temperatures, resulting in broader mesophases.

Our current results suggest that introducing a second functional group provides a useful method for tuning the phase behavior of ester and acid derivatives; LC phase ranges were broadened through significant suppression of the melting temperature and a slight elevation of the clearing temperature in the absence of hydrogen bonding. It is not clear whether these perturbations are a general effect of installing an adjacent substituent next to the carbonyl or is specific to the ether and alcohol groups examined herein. We are continuing to investigate the multi-group interactions to better understand these effects.

Supplementary data

Supplementary data are available with the article through the journal Web site at http://nrcresearchpress.com/doi/suppl/10.1139/cjc-2020-0060.

Acknowledgements

We gratefully acknowledge the Natural Sciences and Engineering Research Council of Canada (NSERC) and Simon Fraser University (SFU) for funding. This work made use of the 4D Labs shared facilities supported by the Canada Foundation for Innovation (CFI), British Columbia Knowledge Development Fund (BCKDF), Western Economic Diversification (WD), and SFU.

References

(1) Wuest, J. D. *Chem. Commun.* **2005**, 5830. doi:10.1039/B512641J.
(2) Goodby, J. W. *Liq. Cryst.* **2017**, *44* (12–13), 1755. doi:10.1080/02678292.2017.1347293.
(3) Goodby, J. W.; Collings, P. J.; Kato, T.; Tschierske, C.; Gleeson, H.; Ranes, P.; Vill, V. *Handbook of Liquid Crystals*. Vol. 1. Wiley-VCH, Weinheim, 2014.
(4) Geelhaar, T.; Griesar, K.; Reckmann, B. *Angew. Chem. Int. Ed.* **2013**, *52* (34), 8798. doi:10.1002/anie.201301457.
(5) Kato, T.; Uchida, J.; Ichikawa, T.; Sakamoto, T. *Angew. Chem. Int. Ed.* **2018**, *57*, 4355. doi:10.1002/anie.201711163.
(6) Thorley, K. J.; Finn, T. W.; Jarolimek, K.; Anthony, J. E.; Risko, C. *Chem. Mater.* **2017**, *29* (6), 2502. doi:10.1021/acs.chemmater.6b04211.
(7) Sutton, C.; Risko, C.; Brédas, J.-L. *Chem. Mater.* **2016**, *28* (1), 3. doi:10.1021/acs.chemmater.5b03266.
(8) Ester, D. F.; McKearney, D.; Herasymchuk, K.; Williams, V. E. *Materials (Basel)* **2019**, *12* (14), 2314. doi:10.3390/ma12142314.
(9) Nafee, S. S.; Hagar, M.; Ahmed, H. A.; El-Shishtawy, R. M.; Raffah, B. M. *Molecules* **2019**, *24*, 3032. doi:10.3390/molecules24173032.
(10) Kumar, M.; Kumar, S. *Polym. J.* **2017**, *49* (1), 85. doi:10.1038/pj.2016.109.
(11) Wöhrle, T.; Wurzbach, I.; Kirres, J.; Kostidou, A.; Kapernaum, N.; Litterscheidt, J.; Haenle, J. C.; Staffeld, P.; Baro, A.; Giesselmann, F., et al. *Chem. Rev.* **2016**, *116* (3), 1139. doi:10.1021/acs.chemrev.5b00190.
(12) Gupta, R. K.; Manjuladevi, V.; Karthik, C.; Choudhary, K. *Liq. Cryst.* **2016**, *43* (13–15), 2079. doi:10.1080/02678292.2016.1195454.
(13) Kumar, S. *Chem. Soc. Rev.* **2006**, *35* (1), 83. doi:10.1039/B506619K.
(14) Bushby, R. J.; Kelly, S. M.; O'Neill, M. *Liquid crystalline semiconductors, materials, properties and applications*. Springer, Dordrecht, 2013; Vol. 169.
(15) Kaafarani, B. R. *Chem. Mater.* **2011**, *23* (3), 378. doi:10.1021/cm102117c.
(16) Wu, J.; Takeda, T.; Hoshino, N.; Suzuki, Y.; Kawamata, J.; Akutagawa, T. *J. Phys. Chem. C* **2019**, *123* (36), 22439. doi:10.1021/acs.jpcc.9b03866.
(17) Takezoe, H. *Mol. Cryst. Liq. Cryst.* **2017**, *646* (1), 46. doi:10.1080/15421406.2017.1284377.
(18) Bose, T. K.; Saha, J. *Phys. Rev. E* **2015**, *92*, 042503. doi:10.1103/PhysRevE.92.042503.
(19) Goossens, K.; Lava, K.; Bielawski, C. W.; Binnemans, K. *Chem. Rev.* **2016**, *116*, 4643. doi:10.1021/cr400334b.
(20) Binnemans, K. *Chem. Rev.* **2005**, *105* (11), 4148. doi:10.1021/cr0400919.
(21) Staffeld, P.; Kaller, M.; Ehni, P.; Ebert, M.; Laschat, S.; Giesselmann, F. *Crystals* **2019**, *9* (2), 74. doi:10.3390/cryst9020074.
(22) Szydłowska, J.; Sitkiewicz, A.; Nazaruk, E.; Pociecha, D.; Krzyczkowska, P.; Krówczyński, A.; Gorecka, E. *Soft Matter* **2018**, *14* (11), 2104. doi:10.1039/C7SM02087B.
(23) Voisin, E.; Foster, E. J.; Rakotomalala, M.; Williams, V. E. *Chem. Mater.* **2009**, *21* (14), 3251. doi:10.1021/cm9012443.
(24) Cheng, K. Y.; Lin, C. H.; Tzeng, M. C.; Mahmood, A.; Saeed, M.; Chen, C.-h.; Ong, C. W.; Lee, S. L. *Chem. Commun.* **2018**, *54* (58), 8048. doi:10.1039/C8CC04241A.
(25) Voisin, E.; Williams, V. E. *Can. J. Chem.* **2018**, *96* (2), 132. doi:10.1139/cjc-2017-0317.
(26) Ong, C. W.; Hwang, J. Y.; Tzeng, M. C.; Liao, S. C.; Hsu, H. F.; Chang, T. H. *J. Mater. Chem.* **2007**, *17* (18), 1785. doi:10.1039/b617827h.
(27) Lavigueur, C.; Foster, J. E.; Williams, V. E. *Liq. Cryst.* **2007**, *34* (7), 833. doi:10.1080/02678290701407243.
(28) Yoshida, J.; Bozek, K. J. A.; Thompson, R.; Williams, V. E. *Soft Matter* **2019**, *15*, 10035. doi:10.1039/C9SM01435G.
(29) Lavigueur, C.; Foster, E. J.; Williams, V. E. *J. Am. Chem. Soc.* **2008**, *130* (35), 11791. doi:10.1021/ja803406k.
(30) Cammidge, A. N.; Jackson, D. J. B. *Philos. Trans. R. Soc. A* **2006**, *364*, 2697. doi:10.1098/rsta.2006.1847.
(31) Foster, J. E.; Lavigueur, C.; Ke, Y. C.; Williams, V. E. *J. Mater. Chem.* **2005**, *15* (37), 4062. doi:10.1039/b503310a.
(32) Foster, E. J.; Jones, R. B.; Lavigueur, C.; Williams, V. E. *J. Am. Chem. Soc.* **2006**, *128* (26), 8569. doi:10.1021/ja0613198.
(33) Bozek, K. J. A.; Ho, K. I.; Saint-Martin, T.; Argyropoulos, P.; Williams, V. E. *Materials (Basel)* **2015**, *8* (1), 270. doi:10.3390/ma8010270.
(34) Wheeler, S. E. *Acc. Chem. Res.* **2013**, *46* (4), 1029. doi:10.1021/ar300109n.
(35) Mohr, B.; Enkelmann, V.; Wegner, G. *J. Org. Chem.* **1994**, *59* (3), 635. doi:10.1021/jo00082a022.
(36) He, R.; Bai, Y.; Yu, Z. H.; Wu, L.; Gunawan, A. M.; Zhang, Z. Y. *Medchemcomm* **2014**, *5* (10), 1496. doi:10.1039/C4MD00099D.
(37) Lu, Y.; Li, Y.; Zhang, R.; Jin, K.; Duan, C. *Tetrahedron* **2013**, *69* (45), 9422. doi:10.1016/j.tet.2013.08.076.
(38) Lehmann, M.; Dechant, M.; Lambov, M.; Ghosh, T. *Acc. Chem. Res.* **2019**, *52* (6), 1653. doi:10.1021/acs.accounts.9b00078.